

## Clinicopathological assessment of cancer/testis antigens NY-ESO-1 and MAGE-A4 in osteosarcoma

Kazuhiko Hashimoto, Shunji Nishimura, Tomohiko Ito, Naohiro Oka, Ryosuke Kakinoki, Masao Akagi

Department of Orthopedic Surgery, Kindai University Hospital, Osaka-Sayama City, Osaka, Japan

### ABSTRACT

The cancer/testis antigens (CTAs), New York esophageal squamous cell carcinoma-1 (NY-ESO-1) and melanoma antigen gene (MAGE)-A4 are normally restricted to male germ cells but are aberrantly expressed in several cancers. Considering the limited information regarding their significance in osteosarcoma (OS), the purpose of this study was to determine the clinical significance of NY-ESO-1 and MAGE-A4 expression in OS. Nine patients with OS treated at Kindai University Hospital were included in the study. The median age was 27 years, and median follow-up period was 40 months. The specimens obtained at the time of biopsy were used to perform immunostaining for NY-ESO, MAGE-A4, p53, and Ki-67. The positive cell rates and positive case rates of NY-ESO, MAGE-A4, p53, and Ki-67 were calculated. The correlation between the positive cell rate of immunohistochemical markers was also calculated. The correlation between the positive cell rate of NY-ESO-1 or MAGE-A4 and tumor size or maximum standardized uptake (SUV-max) was also determined. The positive cell rates of NY-ESO-1 or MAGE-A4 in continuous disease-free (CDF) cases were also compared with those in alive with disease (AWD) or dead of disease (DOD) cases. The average positive cell rates of NY-ESO, MAGE-A4, p53, and Ki-67 were 71.7%, 85.1%, 16.2%, and 14.7%, and their positive case rates were 33.3%, 100%, 44.4%, and 100%, respectively. The positivity rates of NY-ESO-1 and p53 were strongly correlated, whereas those of NY-ESO-1 and Ki-67 were moderately correlated. The MAGE-A4 and p53 positivity rates and the MAGE-A4 and Ki-67 positive cell rates were both strongly correlated. The NY-ESO-1 and MAGE-A4 positivity rates were moderately correlated. The positive correlation between the NY-ESO-1 positive cell rate and tumor size was medium, and that between the MAGE-A4 positivity rate and SUV-max was very strong. There was no significant difference in the positive cell rates of NY-ESO-1 or MAGE-A4 between CDF cases and AWD or DOD cases. Overall, our results suggest that NY-ESO-1 and MAGE-A4 may be involved in the aggressiveness of OS.

**Key words:** New York esophageal squamous cell carcinoma-1 (NY-ESO-1); melanoma antigen gene (MAGE)-A4; osteosarcoma; prognosis; cancer/testis antigen (CTA); immunohistochemistry.

**Correspondence:** Kazuhiko Hashimoto, Department of Orthopedic Surgery, Kindai University Hospital, Osaka-Sayama City, Osaka 589-8511, Japan. Tel. +81.072.3660221 - Fax: +81.072.3660206.  
E-mail: hazzhiko@med.kindai.ac.jp

**Contributions:** KH, SN, NO, MA, conceptualization; KH, SN, TI, RK, MA, methodology; KH, RK, SN, software; SN, NS, NO, RK, MA, validation; SN, NS, NO, TI, MA, formal analysis; KH, TI, NO, RK, SN, investigation; KH, SN, TI, NO, RK, MA, data curation, original draft preparation, review and editing. All the authors read and approved the final version of the manuscript and agreed to be accountable for all aspects of the work.

**Ethics approval and informed consent:** This study complied with the Declaration of Helsinki and was approved by the Ethics Committee of Kindai University Hospital (approval number: R03-021, Osaka, Japan; approval date: April 27, 2021). Written informed consent was obtained from the patients. Comprehensive consent was obtained for patients who were unable to sign.

**Patient consent for publication:** Written informed consent was obtained from the patients for publication of this paper.

**Available data and materials:** The datasets used and/or analyzed during the current study are available from the corresponding author upon reasonable request.

**Conflict of interest:** The authors declare that they have no competing interests, and all authors confirm accuracy.

## Introduction

Osteosarcoma (OS) is one of the most common malignancies of the bones, mainly occurring in children and adolescents, and has potential for local invasion and early metastasis.<sup>1</sup> Despite intensified conventional chemotherapy and surgery, the 5-year survival rate for patients with localized tumors has plateaued at approximately 65%, and for patients with recurrent or metastatic disease, it is approximately 20%.<sup>2,3</sup> Since the 1980s, the outcomes for patients with localized OS have hardly improved. Therefore, additional therapeutic strategies are needed for patients with recurrent tumors and as adjuvants for localized disease.

Cancer/testis antigens (CTAs) are a group of tumor antigens whose normal expression is restricted to male germ cells in the testis and is not found in adult somatic tissues.<sup>4</sup> In addition to their tissue-specific expression profile, the common features of CTAs include their presence as a multigene family, frequent mapping to the X chromosome, induction of expression by hypomethylation and histone acetylation, immunogenicity in cancer patients, heterogeneous protein expression in various tumor types, and likely correlation with tumor progression.<sup>4</sup> Notably, the CTA epitope is recognized by autologous T lymphocytes targeting cancer cells. Therefore, in the last decade, CTAs have emerged as a therapeutic target in cases of malignant disease.<sup>5</sup>

New York esophageal squamous cell carcinoma-1 (NY-ESO-1) is an immunogenic CTA associated with innate and vaccine-induced immunity, which may lead to clinical cancer responses.<sup>6</sup> Abnormal expression of NY-ESO-1 has been reported in various neoplasms including hepatocellular carcinoma, esophageal cancer, melanoma, and non-small cell lung cancer.<sup>7</sup>

The melanoma antigen gene (MAGE) protein family is a large, highly conserved group of proteins with a common MAGE homology domain.<sup>8</sup> MAGE-A is a CTA and a Type I MAGE, which in humans includes members of the MAGE-A, MAGE-B, and MAGE-C subfamilies clustered on the X chromosome.<sup>9</sup> Although the expression of many MAGE proteins is restricted to reproductive tissues similar to NY-ESO, they have been reported to be aberrantly expressed in various cancers. Among MAGEs, MAGE-A4 is widely expressed in many tumor types, including esophageal (60%), ovarian (47%), lung (19-35%), colorectal (22%), and breast (13%) cancers.<sup>8,9</sup>

The tumor suppressor gene *TP53* and its protein product p53 are known to play a major role in cancer progression and suppression, as they are mutated in several cancers.<sup>10</sup> p53 is a transcription factor that promotes the expression of proteins responding to cellular stresses such as hypoxia, viral infection, metabolic stress, endoplasmic reticulum stress, and oxidative stress.<sup>11,12</sup> As cellular stress is one of the causes of cancer, p53 is presumed to inhibit cancer development and progression by modulating stress responses.<sup>11,12</sup> The p53 protein is mutated in more than half of all cancers.<sup>13,14</sup> The significance of p53 in OS pathogenesis has also been reported.<sup>13,14</sup> Interestingly, the overall frequency of p53 mutations in patients with OS is as high as 22%.<sup>15,16</sup>

Furthermore, Ki-67 monoclonal antibodies, which are specific for nuclear antigens expressed throughout the cell cycle (G<sub>1</sub>, S-G<sub>2</sub>, M), but not in quiescent cells (G<sub>0</sub>), have been proposed as valuable resources in the analysis of cancer tissues.<sup>17</sup> Ki-67 immunostaining does not require any preliminary incubation with DNA precursors and allows easy and rapid evaluation of tumor samples.

Although the expression of NY-ESO-1 and MAGE-A4 has been reported in OS, their clinical significance remains unclear.<sup>18,19</sup> Therefore, the current study aimed to identify the clinical significance of NY-ESO-1 and MAGE-A4 in OS using pathological specimens from patients treated at our department, comparing the pathological findings associated with p53 and Ki-67.

## Materials and Methods

### Patient characteristics

Nine patients with OS were included in the current study (Table 1). All the patients were treated in our hospital between March 2012 and March 2017. The current study was approved by the Kindai University Ethics Committee (approval number: R03-021; approved on April 27, 2021). Written informed consent was obtained from the patients. Comprehensive consent was obtained for patients who were unable to sign. The summary data are presented in Table 1. The average age of the patients was 28.5±15.4 years (average±SD, range; 13-52 years). The median follow-up period was 40 months (range; 16-84 months). The site of the lesion was the tibia in three cases, the femur in two cases, the pelvis in two cases, the humerus in one case, and the sacrum in one case. Based on the histopathological types, there were five cases of conventional OS, two cases of chondroblastic type OS, one case of osteoblastic type OS, and one case of fibroblastic type OS. Magnetic resonance imaging (MRI) was used to measure the longest diameter of the tumor in its largest plane; the median tumor length was 11 (range: 4.9-17.5) cm. The maximum standardized uptake (SUV-max) was obtained in six patients and the mean value was 10.08 (range: 2.09-13.9). Based on the Enneking stage<sup>20</sup> at the initial visit, three patients were at stage IIA and six were at stage IIB. Six patients were treated with chemotherapy and wide resection, one patient underwent heavy particle radiation (HPR), one patient underwent chemotherapy and HPR, and one patient underwent chemotherapy and marginal resection. Based on the chemotherapy protocol, seven patients were treated using the neoadjuvant chemotherapy for OS (NECO)-95J protocol,<sup>21</sup> which included doxorubicin, ifosfamide, cisplatin, methotrexate, and one patient was treated with a protocol including ifosfamide and doxorubicin.<sup>22</sup> Two cases of local recurrence were observed after treatment. Three cases of metastasis after treatment were also observed. The outcome at the final observation was six continuous disease-free (CDF) cases, two alive with disease (AWD) cases, and one dead of disease (DOD) case.

### Immunohistochemical staining

Immunostaining for PD-1, PD-L1, NY-ESO, and MAGE-A4 was performed on pathological specimens harvested at the time of biopsy from patients with OS (n=9) who were treated at our institution. Tissue sections were formalin-fixed and paraffin-embedded. Sections of 4 µm thickness were cut and mounted onto slides. The tissues were deparaffinized, rehydrated, and subjected to endogenous peroxidase inhibition using 3% hydrogen peroxide. Antigen retrieval was performed using antigen-specific heat treatments at pH 9 as follows: NY-ESO at 100°C for 64 min; MAGE-A4, at 95°C for 36 min; p53 at 95°C for 64 min; and Ki-67 at 95°C for 64 min. Following heat activation, the tissue sections were incubated with the following primary antibodies: NY-ESO-1 antibody (mouse monoclonal, E978, dilution 1:100; Santa Cruz Biotechnology, Santa Cruz, CA, USA) for 32 min at 37°C; MAGE-A4 antibody (rabbit monoclonal, ab229011, dilution 1:100; Abcam, Cambridge, UK) for 16 min at 37°C; p53 antibody (mouse monoclonal, 7902912, dilution 1:200; Roche Diagnostics, Risch-Rotkreuz, Switzerland) for 16 min at 37°C; Ki-67 antibody (mouse monoclonal, M7240; dilution 1:200; Agilent Technology, CA, USA) for 16 min at 37°C. As the secondary antibodies, goat anti-mouse IgG+IgM H&L (HRP) preadsorbed (ab47827, dilution 1:500; Abcam) was used for NY-ESO-1, goat anti-rabbit IgG H&L (HRP) preadsorbed (ab7090, dilution 1:1000; Abcam) was used for MAGE-A4, rabbit anti-mouse IgG H&L (HRP) (ab6728, dilution 1:500; Abcam) was used for p53 and Ki-67 for incubation at 37°C.

The reaction was visualized using 3,3-diaminobenzidine (DAB Substrate Chromogen System; DAKO, Kyoto, Japan) and the sections were counterstained with hematoxylin. Testes were used as positive controls for NY-ESO and MAGE-A4, respectively. In all immunohistochemical staining experiments, negative control experiments were performed using IgG adapted for each stain to check for nonspecific binding. The slides were observed under a microscope (BIOREVO BZ-9000; Keyence, Osaka, Japan), and brown granules in the cytoplasm or nuclei indicated positive staining. Immune marker staining within the tumor was quantified in four representative high-power fields (40× magnification).<sup>23</sup> The positivity rate for each immune component was then calculated. The positivity rate was defined as the number of positive cells/total cell number, and was quantified using BIOREVO-BZ 9000 software (Keyence).

### Correlation between the positive cell rates of immunohistochemical markers and the correlation between the positive cell rate of NY-ESO-1 or MAGE-A4 and tumor size and clinical features

Further, a positive rate ≥5% was considered a positive case, and the percentage of positive cases for each immunohistochemical marker was calculated. The correlations between the positive cell rates of each immunohistochemical marker were examined. The correlations between tumor size (longest diameter on MRI) and positive cell rates for each immunohistochemical marker were examined. The correlations between the SUV-max value and positive cell rates of each immunohistochemical marker were examined.<sup>23</sup>

### Comparison of positive cell rates for each marker in remission cases with those in non-remission cases

The positive cell rates of various markers were also compared between patients who were in remission (CDF cases) and those who were not in remission (AWD or DOD cases).

### Statistical analysis

The positivity rate of each marker was plotted, and a correlation diagram was drawn.<sup>23</sup> The coefficient of determination (R) was calculated by drawing an approximation line to examine the correlation between each marker. Pearson's method of testing for correlations was used to perform the tests. The correlation between clinical parameters and the positive rate of each molecule was also investigated in a similar manner. We determined  $1.0 \geq |r| \geq 0.7$  as very strong,  $0.7 \geq |r| \geq 0.5$  as strong,  $0.5 \geq |r| \geq 0.4$  as moderate,  $0.4 \geq |r| \geq 0.3$  as medium,  $0.3 \geq |r| \geq 0.2$  as weak, and  $0.2 \geq |R| \geq 0.0$  as no correlation.<sup>2</sup> Binary logistic analysis was used to test the significance of the correlations. The chi-square test was used to compare the cases in remission with the non-remission cases;  $p < 0.05$  was considered statistically significant. Analyses were performed using Stat Mate 5.05 (ATMS, Tokyo, Japan).

## Results

### The positive cell rate of each immunohistochemical marker

Representative images for the positive staining of NY-ESO, MAGE-A4, p53, and Ki-67 are shown in Figure 1A–D. NY-ESO and MAGE-A4 were stained in the cytoplasm whereas p53 and Ki-67 were stained in the nuclei. The positive cell rates of NY-ESO, MAGE-A4, p53, and Ki-67 are shown in Table 1. The average positive cell rates of NY-ESO, MAGE-A4, p53, and Ki-67 were 71.7%, 85.1%, 16.2%, and 14.7%, respectively.

**Table 1. Positive rates of NY-ESO, MAGE-A4, p53, and Ki-67, and the clinical features of patients with primary osteosarcoma treated at our hospital.**

Patient no.	Age (y)	Sex	Site	Histopathological type	Tumor size (cm)	SUV-max value	Stage	Treatment	Chemotherapy	Local recurrence	Metastasis (after treatment)	Follow-up (months)	Outcome	NY-ESO (positive rate, %)	MAGE-A4 (positive rate, %)	p53 (positive rate, %)	Ki-67 (positive rate, %)
1	13/F	F	Femur	Conventional	14 x 7.5	-	IIB	CT, WR	NECO-95J	-	-	65	CDF	0	50.8	0	7.41
2	15/F	F	Femur	Osteoblastic	11 x 3.5	-	IIB	CT, WR	NECO-95J	-	-	84	CDF	0.25	85.1	0	7.95
3	32/M	M	Pelvis	Conventional	11 x 7.2	10.5	IIB	HPR, DXR, IFO, CDDP, MTX	NECO-95J	N/A	+	55	AWD	0.1	96.6	0	5.47
4	14/M	M	Tibia	Conventional	16 x 8.6	9.66	IIB	CT, WR	NECO-95J	-	-	24	CDF	0	88.2	19.2	10.2
5	52/M	M	Pelvis	Conventional	6.6 x 3	12.13	IIA	CT, WR	NECO-95J	+	+	32	AWD	0	34.8	15.4	26.9
6	36/F	F	Tibia	Chondroblastic	5.9 x 5.5	13.83	IIA	CT, WR	NECO-95J	-	-	40	CDF	0	56.1	1.3	14.6
7	51/M	M	Humerus	Fibroblastic	5.3 x 4	2.09	IIA	CT, MR	IA	-	-	44	CDF	37.9	47	10.7	5
8	16/M	M	Tibia	Conventional	17.5 x 3.8	-	IIB	CT, WR	NECO-95J	-	-	39	CDF	19.2	96.6	100	41
9	27/F	F	Sacrum	Chondroblastic	4.9 x 2.7	4.89	IIB	CT, HPR	NECO-95J	N/A	+	16	DOD	7.1	94.9	0	13.8

y, years; F, female; M, male; DM, diabetes mellitus; SUV-max, maximum standardized uptake; CT, chemotherapy; WR, wide resection; MR, marginal resection; mo, month(s); HPR, heavy particle radiation; NECO-95, neoadjuvant chemotherapy for osteosarcoma in Japan-95; N/A, not applicable; CDF, continuously disease-free; NED, no evidence of disease; DOD, dead of disease; AWD, alive with disease; IA, doxorubicin/ifosfamide.

### Immunohistochemical positive case rate of each marker

The positive case rate of NY-ESO, MAGE-A4, p53, and Ki-67 was 3/9 (33.3%), 9/9 (100%), 4/9 (44.4%), and 9/9 (100%), respectively.

### Correlation between the positive cell rates of immunohistochemical markers

The positive correlation between the NY-ESO-1 and p53 positivity rates was strong ( $r = 0.52$ ,  $p=0.90$ , Figure 2A), whereas that between the NY-ESO-1 and Ki-67 positivity rates was moderate ( $r = 0.45$ ,  $p=0.60$ , Figure 2B). The positive correlation between MAGE-A4 and p53 rates was strong ( $r = 0.52$ ,  $p=0.89$ , Figure 2C). The positive correlation between MAGE-A4 and Ki-67 positivity rates was also strong ( $r = 0.77$ ,  $p=0.72$ , Figure 2D). The positive correlation between the NY-ESO-1 and MAGE-A4 positivity rates was moderate ( $r = 0.44$ ,  $p=0.38$ , Figure 2E). The positive correlation between the p53 and Ki-67 positivity rates was very strong ( $r = 0.85$ ,  $p=0.13$ , Figure 2F).

### Correlation between the positive cell rate of NY-ESO-1 or MAGE-A4 and tumor size

Interestingly, the positive correlation between the NY-ESO-1 positivity rate and tumor size was medium ( $r = 0.39$ ,  $p=0.53$ , Figure 3A), whereas that between the MAGE-A4 positivity rate and tumor size was very strong ( $r = 0.92$ ,  $p=0.30$ , Figure 3B).

### Correlation between the positive cell rate of NY-ESO-1 or MAGE-A4 and SUV-max

The NY-ESO-1 positive cell rate and SUV-max value was not correlated ( $r = 0.12$ ,  $p=0.66$ , Figure 3C), whereas the positive correlation between MAGE-A4 positivity rate and SUV-max value was very strong ( $r = 0.83$ ,  $p=0.74$ , Figure 3D).

### The positive cell rate of NY-ESO-1 or MAGE-A1 in CDF cases with AWD or DOD cases

The positive cell rate of NY-ESO-1 in CDF cases and in AWD or DOD cases was  $7.63 \pm 16.9$  and  $6.6 \pm 9.03$ , (average  $\pm$ SD), respectively, and showed no significant difference between ( $p=0.91$ ). The

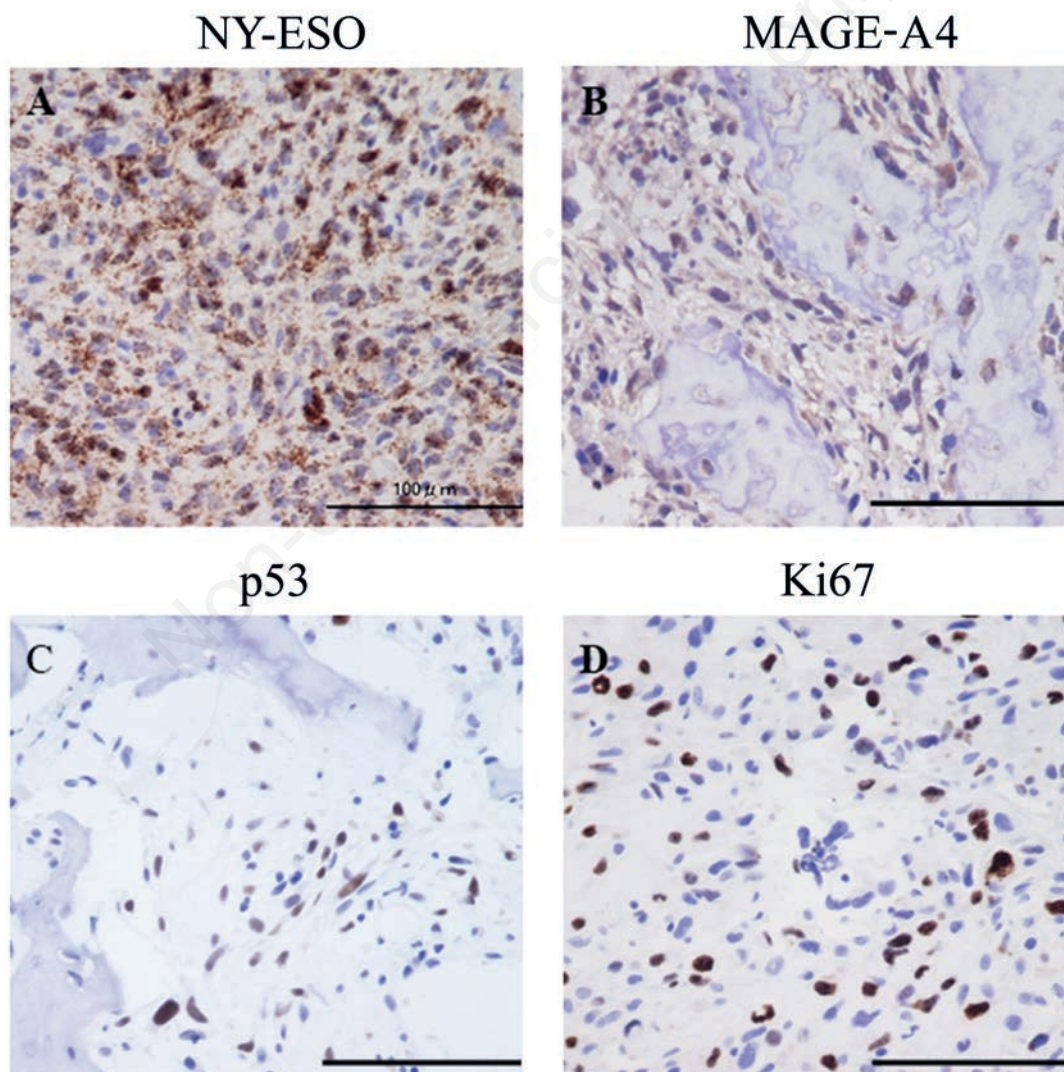


**Figure 1.** Immunostaining for New York esophageal squamous cell carcinoma (NY-ESO), melanoma antigen gene (MAGE)-A4, p53, and Ki-67 (A-D). Representative images showing staining for NY-ESO-1 (A), MAGE-A (B), p53 (C), and Ki-67 (D). NY-ESO-1 (A) and MAGE-A4 (B) were positive in the cytoplasm, whereas p53 (C) and Ki-67 (D) were positive in the nucleus. Scale bars: 100 µm.

positive cell rate of MAGE-A4 in CDF cases and in AWD or DOD cases was  $65.4 \pm 19.6$  and  $80.7 \pm 30.6$ , (average  $\pm$ SD), respectively, and showed no significant difference ( $p=0.39$ ). The values of  $r$  and  $p$ -values are summarized in Table 2.

## Discussion

In this study, we investigated the involvement of NY-ESO-1 and MAGE-A4 in the clinical pathogenesis of OS using p53 and Ki-67 immunostaining. Previous studies have shown that the positive rates of NY-ESO-1 in OS are 0–31.3%.<sup>19,24</sup>

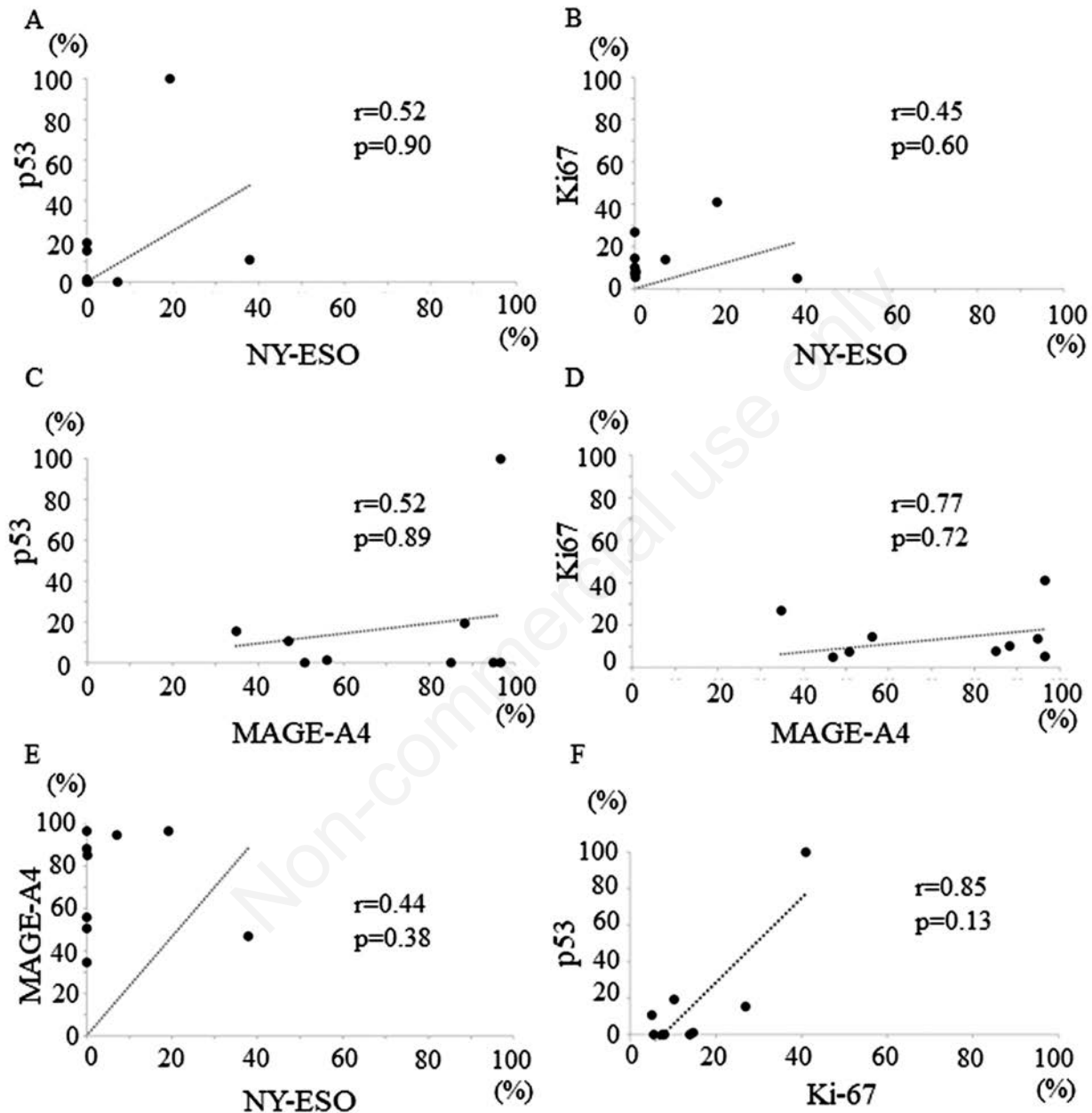


**Figure 2.** Correlation between positive cell rates of immunohistochemical markers (A-D). A) Correlation between positive cell rates of New York esophageal squamous cell carcinoma-1 (NY-ESO-1) and p53. B) Correlation between positive cell rates of NY-ESO-1 and Ki-67; the positive correlation between NY-ESO-1 and p53 positive cell rates was strong ( $r=0.52$ ,  $p=0.90$ ); furthermore, the positive correlation between the NY-ESO-1 and Ki-67 positive cell rates was moderate ( $r=0.45$ ,  $p=0.60$ ). C) Correlation between positive cell rates of melanoma antigen gene (MAGE)-A4 and p53. D) Correlation between positive cell rates of MAGE-A4 and Ki-67; the positive correlation between positive cell rates of MAGE-A4 and p53 was strong ( $r=0.52$ ,  $p=0.89$ ); further, the positive correlation between MAGE-A4 and Ki-67 positive cell rates was also strong ( $r=0.77$ ,  $p=0.72$ ). E) Correlation between positive cell rates of NY-ESO-1 and MAGE-A4; the correlation between the NY-ESO-1 and MAGE-A4 positive cell rates was moderate ( $r=0.44$ ,  $p=0.38$ ). F) Correlation between the positive cell rates of p53 and Ki-67; the correlation between the NY-ESO-1 and MAGE-A4 positive cell rates was moderate ( $r=0.85$ ,  $p=0.13$ ).

In the current study, the positive rate of NY-ESO-1 was 33.3% (3/9), which was higher than that reported in previous studies. Further compared to the positive rate of MAGE-A4 reported in a previous study as 43.8%,<sup>19</sup> the positive rate of MAGE-A4 in the current study was 100% (9/9), which was much higher. Further, a previous study showed that the positive rate of both NY-ESO-1 and MAGE-A4 was 25%,<sup>1</sup> whereas in the current study, the posi-

tive rate of both NY-ESO-1 and MAGE-A4 was 33.3% (3/9), which was higher than the previously reported value. The reason for the high rate of positivity compared to previous studies is that only immunostaining was evaluated. Additional studies at the DNA and protein levels will be required in the future. However, these findings suggest the involvement of NY-ESO-1 and MAGE-A4 in OS pathogenesis.

**Table 2.** The correlation between immune molecules and clinical features.

X-axis	NY-ESO-1	NY-ESO-1	MAGE-A4	MAGE-A4	NY-ESO-1	Ki-67	NY-ESO-1	MAGE-A4	NY-ESO-1	MAGE-A4
Y-axis	p53	Ki-67	p53	Ki-67	MAGE-A4	p53	Size	Size	SUV-max	SUV-max
r	0.52	0.45	0.52	0.77	0.44	0.85	0.39	0.92	0.12	0.83
p	0.90	0.60	0.89	0.72	0.38	0.13	0.53	0.30	0.66	0.74

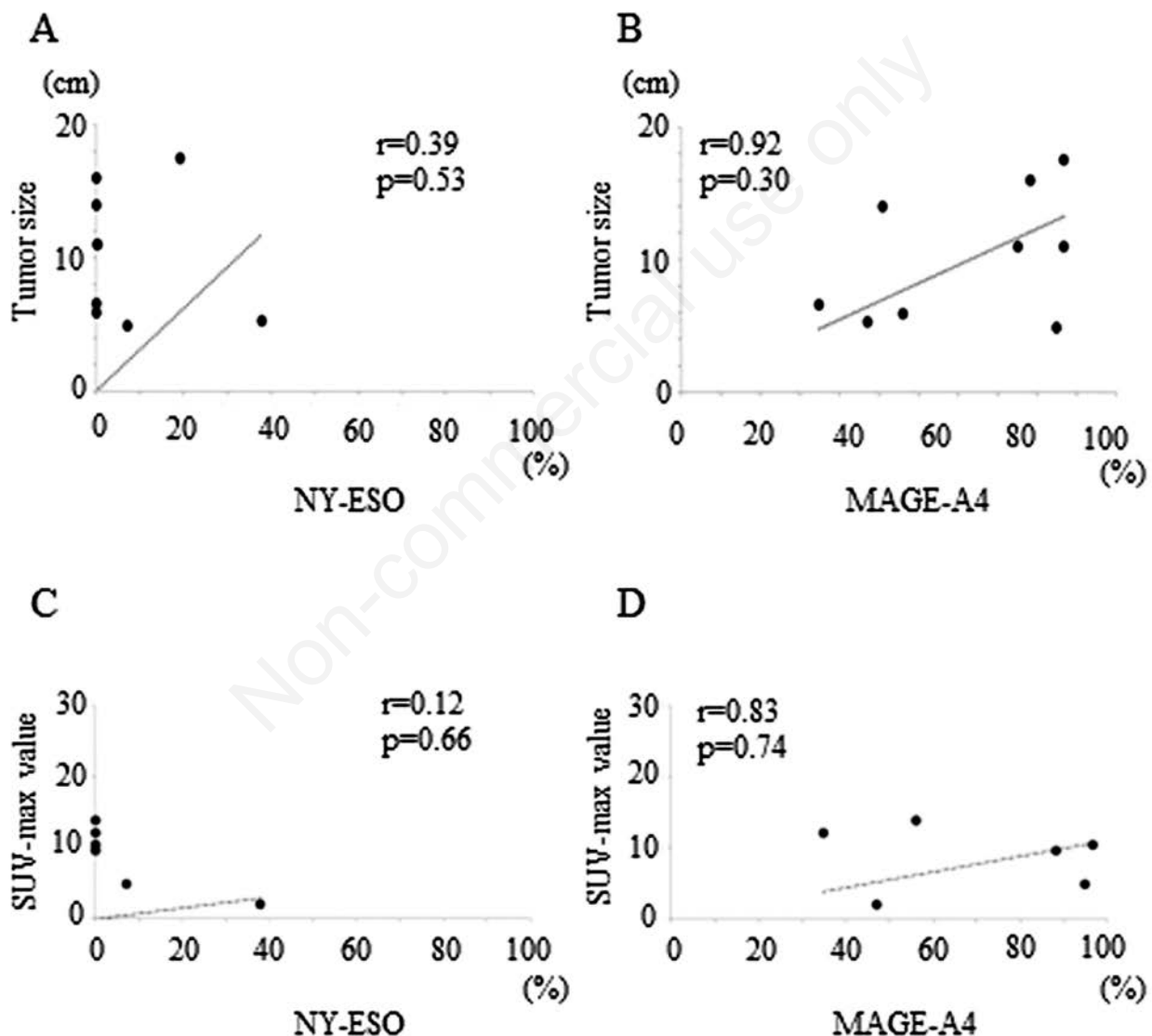


**Figure 3.** The positive correlation between the positive cell rate of New York esophageal squamous cell carcinoma-1 (NY-ESO-1) or melanoma antigen gene (MAGE)-A4 and tumor size (A,B). A medium positive correlation was found between the NY-ESO-1 positive cell rate and tumor size ( $r=0.39$ ,  $p=0.53$ , A). The positive correlation between the MAGE-A4 positive cell rates and tumor size was very strong ( $r=0.92$ ,  $p=0.30$ , B). Positive correlation between the positive cell rate of NY-ESO-1 or MAGE-A4 and SUV-max (C and D). The NY-ESO-1 positive cell rate and SUV-max value was not correlated ( $r=0.12$ ,  $p=0.66$ ), and the positive correlation between the MAGE-A4 positive cell rates and SUV-max value was very strong ( $r=0.83$ ,  $p=0.74$ ).

p53 mutations have also been associated with pathological grade and survival and have been reported as a potential prognostic biomarker for OS.<sup>25,26</sup> In the current study, p53 expression was positively correlated with that of NY-ESO-1 and MAGE-A4, suggesting their potential as prognostic biomarkers for OS. Ki-67 is also a well-known marker for assessing cell proliferation and invasion,<sup>27-29</sup> and has been reported as a marker for diagnosis of malignancy, proliferation, response to chemotherapy, and prognosis in OS.<sup>29,30</sup> In the current study, Ki-67 expression was a positively correlated NY-ESO and MAGE-A4 suggesting their potential as markers for the diagnosis of malignancy, proliferation, response to chemotherapy, and prognosis for OS. Coexistence of p53 and Ki-67 represents high-grade OS and poor prognosis.<sup>31</sup> In the present study, 4/9 (44.4%) cases were positive for both p53 and Ki-67; they were also positive for MAGE-A4.

Among the various prognostic determinants of OS, tumor size is one of the most important.<sup>3</sup> In this study, we found a positive correlation between tumor size and NY-ESO/MAGE-A4 positivity, indicating that NY-ESO/MAGE-A4 positivity may help predict OS tumor growth. However, it should also be kept in mind that the treatment may correlate with the treatment and not with the immune effect of CTA, as treatment varies from case to case.

SUV-max, the most used parameter for measuring the metabolic activity of tumors,<sup>33</sup> has been reported as a biomarker for predicting survival in OS, the likelihood of metastasis, and response to chemotherapy.<sup>34,36</sup> Here, we found that MAGE-A4 expression was correlated with the SUV-max value, suggesting that MAGE-A4 may be considered a biomarker for metastasis, and response to chemotherapy in OS.

To the best of our knowledge, the involvement of NY-ESO-1 or MAGE-A4 in the prognosis of OS has not been coherently reported to date. In this study, we found no significant difference in the NY-ESO-1 or MAGE-A4 positivity between CDF patients and AWD or DOD patients. However, additional studies with an increased number of patients for long-term follow-up are necessary in the future.

This study has some limitations. First, the small sample size may have affected the significance of the findings and potency of the statistical results in this study. Although the sample size was also too small to procure significant differences in correlation, the results of this study suggest that NY-ESO-1 and MAGE-A4 are involved in the aggressiveness of OS. Second, there was a possible bias in the correlation between tumor size and CTA positivity rate because the treatment was not identical in all patients. Third, as only immunostaining studies were used here, the expression of NY-ESO-1 and MAGE-A4 at the genetic level was not confirmed. Fourth, we could not investigate the downstream pathway or other immune molecules such as the p53-MDM2 or p16/Rb pathways.<sup>37</sup> Finally, the direct effects of NY-ESO-1 and MAGE-A4 on p53, Ki-67, and the pathogenesis of OS have not been elucidated. Despite these limitations, the current study provides evidence for the involvement of NY-ESO-1 and MAGE-A4 in OS pathogenesis and prognosis. However, further studies with larger sample sizes are required to validate these findings.

Overall, our results suggest that NY-ESO-1 and MAGE-A4 may be involved in OS with aggressive clinical behavior.

## Acknowledgements

*We would like to thank Chikoto Tanaka for providing technical assistance.*

## References

- Eaton BR, Schwarz R, Vatner R, Yeh B, Claude L, Indelicato DJ, Laack N. Osteosarcoma. *Pediatr Blood Cancer* 2021;68:e28352.
- Smrke A, Anderson PM, Gulia A, Gennatas S, Huang PH, Jones RL. Future directions in the treatment of osteosarcoma. *Cells* 2021;10:172.
- Belayneh R, Fourman MS, Bhogal S, Weiss KR. Update on osteosarcoma. *Curr Oncol Rep* 2021;23:71.
- Das B, Senapati S. Immunological and functional aspects of MAGEA3 cancer/testis antigen. *Adv Protein Chem Struct Biol* 2021;125:121-47.
- Florke Gee RR, Chen H, Lee AK, Daly CA, Wilander BA, Fon Tacer K, et al. Emerging roles of the MAGE protein family in stress response pathways. *J Biol Chem* 2020;295:16121-55.
- Raza A, Merhi M, Inchakalody VP, Krishnankutty R, Relecom A, UddinS, et al. Unleashing the immune response to NY-ESO-1 cancer testis antigen as a potential target for cancer immunotherapy. *J Transl Med* 2020;18:140.
- Meng X, Sun X, Liu Z, He Y. A novel era of cancer/testis antigen in cancer immunotherapy. *Int Immunopharmacol* 2021;98:107889.
- Li S, Shi X, Li J, Zhou X. Pathogenicity of the MAGE family. *Oncol Lett* 2021;22:844.
- Saito T, Wada H, Yamasaki M, Miyata H, Nishikawa H, Sato E, et al. High expression of MAGE-A4 and MHC class I antigens in tumor cells and induction of MAGE-A4 immune responses are prognostic markers of CHP-MAGE-A4 cancer vaccine. *Vaccine* 2014;32:5901-7.
- Zhang S, Carlsen L, Hernandez Borrero L, Seyhan AA, Tian X, El-Deiry WS. Advanced strategies for therapeutic targeting of wild-type and mutant p53 in cancer. *Biomolecules* 2022;12:548.
- Cordani M, Butera G, Pacchiana R, Masetto F, Mullappilly N, Riganti C, et al. Mutant p53-associated molecular mechanisms of ROS regulation in cancer cells. *Biomolecule*. 2020;10:361.
- Zhang X, Qi Z, Yin H, Yang G. Interaction between p53 and Ras signaling controls cisplatin resistance via HDAC4- and HIF-1 $\alpha$ -mediated regulation of apoptosis and autophagy. *Theranostics* 2019;9:1096-114.
- Pan Z, Cheng D-D, Wei X-J, Li S-J, Guo H, Yang Q-C. Chitooligosaccharides inhibit tumor progression and induce autophagy through the activation of the p53/mTOR pathway in osteosarcoma. *Carbohydr Polym* 2021;258:117596.
- Nakayama M, Oshima M. Mutant p53 in colon cancer. *J Mol Cell Biol* 2019;11:267-76.
- Thoenen E, Curl A, Iwakuma T. TP53 in bone and soft tissue sarcomas. *Pharmacol Ther* 2019;202:149-64.
- Synoradzki KJ, Bartnik E, Czarnicka AM, Fiedorowicz M, Firlej W, Brodziak A, et al. TP53 in biology and treatment of osteosarcoma. *Cancers* 2021;13:4284.
- Klöppel G, La Rosa S. Ki67 labeling index: assessment and prognostic role in gastroenteropancreatic neuroendocrine neoplasms. *Virchows Arch* 2018;472:341-9. Erratum in: *Virchows Arch* 2018;472:515.
- Miwa S, Shirai T, Yamamoto N, Hayashi K, Takeuchi A, Igarashi K, et al. Current and emerging targets in immunotherapy for osteosarcoma. *J Oncol* 2019;2019:7035045.
- Stein JN, D'Angelo SP. Maximizing immunotherapy in sarcoma using histology, biomarkers and novel approaches. *touchREVIEWS in Oncology & Haematology* 2022;18. Ahead of Print publication
- Zhou C, Qian G, Wang Y, Li H, Yu W, Zheng S, et al. Impact of secondary aneurysmal bone cysts on survival of patients

- with Enneking stage IIB extremity osteosarcoma: A propensity score matching analysis. *Ann Surg Oncol* 2021;12:7864-72.
21. Hiraga H, Ozaki T. Adjuvant and neoadjuvant chemotherapy for osteosarcoma: JCOG bone and soft tissue tumor study group. *Jpn J Clin Oncol* 2021;51:1493-7.
  22. Verma P, Jain S, Kapoor G, Tripathi R, Sharma P, Doval DC. IAP chemotherapy regimen is a viable and cost-effective option in children and adolescents with osteosarcoma: a comparative analysis with MAP regimen on toxicity and survival. *J Pediatr Hematol Oncol* 2021;43:e466-71.
  23. Hashimoto K, Nishimura S, Ito T, Akagi M. Characterization of PD-1/PD-L1 immune checkpoint expression in soft tissue sarcomas. *Eur J Histochem* 2021;65:3203.
  24. Lai JP, Rosenberg AZ, Miettinen MM, Lee CC. NY-ESO-1 expression in sarcomas: A diagnostic marker and immunotherapy target. *Oncoimmunology* 2012;1:1409-10.
  25. Otani S, Ueno T, Ito T, Kajikawa S, Omori K, Taniuchi I, et al. Runx3 is required for oncogenic Myc upregulation in p53-deficient osteosarcoma. *Oncogene* 2022;41:683-91.
  26. Zhou, L, Yu Y, Sun S, Zhang T, Wang M. Cry 1 Regulates the clock gene network and promotes proliferation and migration via the Akt/P53/P21 pathway in human osteosarcoma cells. *J Cancer* 2018;9:2480-91.
  27. Travaglino A, Raffone A, Catena U, De Luca M, Toscano P, Del Prete E, et al. Ki67 as a prognostic marker in uterine leiomyosarcoma: A quantitative systematic review. *Eur J Obstet Gynecol Reprod Biol* 2021;266:119-24.
  28. Davey MG, Hynes SO, Kerin MJ, Miller N, Lowery AJ. Ki-67 as a prognostic biomarker in invasive breast cancer. *Cancers* 2021;13:4455.
  29. Niculescu SA, Grecu DC, Simionescu CE, Niculescu EC, Stepan MD, Stepan AE. Immunoexpression of Ki67, p53 and cyclin D1 in osteosarcomas. *Rom J Morphol Embryol* 2021;62:743-50. doi:10.47162/RJME.62.3.11
  30. Zeng M, Zhou J, Wen L, Zhu Y, Luo Y, Wang W. The relationship between the expression of Ki-67 and the prognosis of osteosarcoma. *BMC Cancer* 2021;21:210.
  31. Siontis BL, McHugh JB, Roberts E, Zhao L, Thomas DG, Owen D, et al. Differential outcomes and biologic markers of radiation-associated vs. sporadic osteosarcoma: a single-institution experience. *Front Oncol* 2020;9:1523.
  32. Xin S, Wei G. Prognostic factors in osteosarcoma: A study level meta-analysis and systematic review of current practice. *J Bone Oncol* 2020;21:100281.
  33. Farina A, Gasperini C, Aparisi Gómez MP, Bazzocchi A, Fanti S, Nanni C. The role of FDG-PET and whole-body MRI in high grade bone sarcomas with particular focus on osteosarcoma. *Semin Nucl Med* 2021;S0001-2998(21)00076-3.
  34. Jeong SY, Kim W, Byun BH, Kong CB, Song WS, Lim I, et al. Prediction of chemotherapy response of osteosarcoma using baseline 18F-FDG textural features machine learning approaches with PCA. *Contrast Media Mol Imaging* 2019;2019:3515080.
  35. Sheen H, Kim W, Byun BH, Kong CB, Song WS, Cho WH, et al. Metastasis risk prediction model in osteosarcoma using metabolic imaging phenotypes: A multivariable radiomics model. *PLoS One* 2019;14:e0225242.
  36. Davis JC, Daw NC, Navid F, Billups CA, Wu J, Bahrami A, et al. 18F-FDG uptake during early adjuvant chemotherapy predicts histologic response in pediatric and young adult patients with osteosarcoma. *J Nucl Med* 2018;59:25-30.
  37. Russell DS, Jaworski L, Kisseberth WC. Immunohistochemical detection of p53, PTEN, Rb, and p16 in canine osteosarcoma using tissue microarray. *J Vet Diagn Invest* 2018;30:504-9.

---

Received for publication: 28 December 2021. Accepted for publication: 16 June 2022.

This work is licensed under a Creative Commons Attribution-NonCommercial 4.0 International License (CC BY-NC 4.0).

©Copyright: the Author(s), 2022

Licensee PAGEPress, Italy

*European Journal of Histochemistry* 2022; 66:3377

doi:10.4081/ejh.2022.3377

*Publisher's note: All claims expressed in this article are solely those of the authors and do not necessarily represent those of their affiliated organizations, or those of the publisher, the editors and the reviewers. Any product that may be evaluated in this article or claim that may be made by its manufacturer is not guaranteed or endorsed by the publisher.*